Journal of Biomechanics 44 (2011) 1805–1809

Contents lists available at ScienceDirect

Journal of Biomechanics

journal homepage: www.elsevier.com/locate/jbiomech
www.JBiomech.com

Short communication

# Kinematic performance of a six degree-of-freedom hand model (6DHand) for use in occupational biomechanics ☆

Frank L. Buczek*, Erik W. Sinsel, Daniel S. Gloekler, Bryan M. Wimer, Christopher M. Warren, John Z. Wu

*National Institute for Occupational Safety and Health (NIOSH), 1095 Willowdale Road MS 2027, Morgantown, WV 26505, United States*

ARTICLE INFO

*Article history:*
Accepted 1 April 2011

*Keywords:*
Biomechanics
Hand
Finger
Model
Six degree-of-freedom
Occupational safety

ABSTRACT

Upper extremity musculoskeletal disorders represent an important health issue across all industry sectors; as such, the need exists to develop models of the hand that provide comprehensive biomechanics during occupational tasks. Previous optical motion capture studies used a single marker on the dorsal aspect of finger joints, allowing calculation of one and two degree-of-freedom (DOF) joint angles; additional algorithms were needed to define joint centers and the palmar surface of fingers. We developed a 6DOF model (6DHand) to obtain unconstrained kinematics of finger segments, modeled as frusta of right circular cones that approximate the palmar surface. To evaluate kinematic performance, twenty subjects gripped a cylindrical handle as a surrogate for a powered hand tool. We hypothesized that accessory motions (metacarpophalangeal pronation/supination; proximal and distal interphalangeal radial/ulnar deviation and pronation/supination; all joint translations) would be small (less than 5° rotations, less than 2 mm translations) if segment anatomical reference frames were aligned correctly, and skin movement artifacts were negligible. For the gripping task, 93 of 112 accessory motions were small by our definition, suggesting this 6DOF approach appropriately models joints of the fingers. Metacarpophalangeal supination was larger than expected (approximately 10°), and may be adjusted through local reference frame optimization procedures previously developed for knee kinematics in gait analysis. Proximal translations at the metacarpophalangeal joints (approximately 10 mm) were explained by skin movement across the metacarpals, but would not corrupt inverse dynamics calculated for the phalanges. We assessed performance in this study; a more rigorous validation would likely require medical imaging.

Published by Elsevier Ltd.

## 1. Introduction

Upper extremity musculoskeletal disorders are recognized as an important occupational health issue across all industry sectors (Marras et al., 2009). Worker's compensation claims in 2006 included $12.4 billion for related over-exertions (Liberty-Mutual, 2008). In manufacturing, shoulder, wrist, hand, and finger disorders accounted for 33% of lost work day injuries (BLS, 2005). Carpal-tunnel-syndrome (CTS) and hand–arm-vibration-syndrome (HAVS) adversely affect workers who use powered hand tools or engage in manual assembly operations, where injury severity is related to gripping mechanics (NIOSH, 1997). The need exists to develop hand models that provide comprehensive biomechanics during occupational tasks.

The metacarpophalangeal joint (MCP) of the index, middle, ring, and little fingers (F2, F3, F4 and F5, respectively) primarily allows flexion/extension and radial/ulnar deviation; the proximal and distal interphalangeal joints (PIP, DIP) primarily allow flexion/extension (Netter, 1991). Clinically defined accessory motions include rotations and translations other than these primary rotations, and are small for normal joints (Kuczynski, 1975). Accessory rotations at the MCP joint include pronation/supination; those at the PIP and DIP joints include radial/ulnar deviation and pronation/supination. Detailed studies of these motions, free from skin movement artifact, are rare. Using a radiographic technique to obtain bone-to-bone motions for two human subjects, Chao et al. (1989, p. 89) reported accessory motions for pinching and grasping tasks (Table 1). Using an electromagnetic tracking system, Minamikawa et al. (1993) reported PIP joint motion for 12 cadaver index fingers. Using a similar technique Uchiyama et al. (2000) reported PIP joint motion for nine cadaver middle fingers, with externally applied moments. Using circular bone wires fixed to each phalange and metacarpal, Degeorges and Oberlin (2003) reported means and standard deviations for

☆ *Disclaimer*: The findings and conclusions in this report are those of the authors and do not necessarily represent the views of the National Institute for Occupational Safety and Health.

* Corresponding author. Tel.: +1 304 285 5966; fax: +1 304 285 6265.
*E-mail address:* fbuczek@cdc.gov (F.L. Buczek).

0021-9290/$ - see front matter Published by Elsevier Ltd.
doi:10.1016/j.jbiomech.2011.04.003

**Table 1**
Summary of accessory rotations reported by others.

| Reference | Method | Source | Comments | Radial/ulnar deviation (PIP, DIP) | Pronation/supination (MCP, PIP, DIP) |
|---|---|---|---|---|---|
| Chao et al. (1989) [Note 1] | In vivo, three-dimensional radiographs | $n=2$ Human subjects | Tip pinch Mean across F2, F3 | 4.6° (magnitude) | 5.7° (magnitude) |
| | | | Grasp 38 mm cylinder Mean across F2–F5 | 6.0° (magnitude) | 6.7° (magnitude) |
| Minamikawa et al. (1993) [Note 2] | Six degree-of-freedom electromagnetic motion capture | $n=12$ Cadaver fingers | Passive, unloaded flexion, F2 PIP only | 5° (ulnar deviation) | 9° (supination) |
| Uchiyama et al. (2000) [Note 2] | Six degree-of-freedom electromagnetic motion capture | $n=9$ Cadaver fingers | Passive, loaded, flexion, F3 PIP only | 5° (radial load) 5° (ulnar load) | 24° (pronation load) 21° (supination load) |
| Degeorges et al. (2003) [Note 3] | Circular bone wires applied via partially dissected skin | $n=22$ Cadaver hands | Passive, unloaded, flexion, mean $\pm\sigma$ across F2–F5 | 5.0° (radial deviation) 5.6° (ulnar deviation) | 3.3° (pronation) 6.1° (supination) |
| Degeorges et al. (2004) [Note 3] | CT scans with fingers taped in full flexion | $n=6$ Cadaver hands | Passive, unloaded, flexion, mean $\pm\sigma$ across F2–F5 | 2.9° (radial deviation) 9.9° (radial deviation) | 5.1° (pronation) 10.3° (supination) |
| Degeorges et al. (2005) [Note 3] | In vivo, six degree-of-freedom Vicon motion capture | $n=6$ Human subjects | Passive, unloaded, flexion, mean $\pm\sigma$ across F2–F5 | 5.4° (radial deviation) 18.6° (radial deviation) | 6.3° (pronation) 2.7° (supination) |

Nomenclature: MCP=metacarpophalangeal joint. PIP/DIP=proximal/distal interphalangeal joints. F2, F3, F4, and F5 refer to index, middle, ring, and little fingers, respectively. Notes: [1] Mean magnitudes are reported here because no standard deviations ($\sigma$) were provided with the means in the associated references; averaging their reported means would produce near zero results. [2] These authors studied only the PIP joint accessory rotations, for a single finger. [3] These authors reported accessory rotations (mean $\pm\sigma$) at the MCP, PIP, and DIP joints for all fingers; data in this table are average lower bounds (mean $-\sigma$), and average upper bounds (mean $+\sigma$), across all fingers and joints, and capture 68% of all observations.

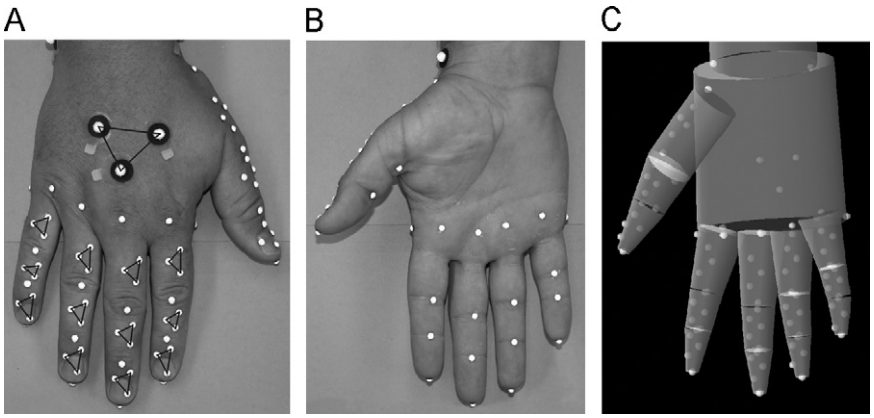


**Fig. 1.** Marker configuration. Calibration markers (4 mm hemispheres) are applied to the dorsal (A) and palmar (B) joint lines to calculate joint centers; three additional dorsal markers (indicated by triangles) track each finger, hand, and forearm (not shown) segment. Frusta of right circular cones (C) approximate the palmar surface of the fingers.

accessory rotations among 22 partially dissected cadaver hands. Using CT scans, Degeorges et al. (2004) reported similar data among six cadaver hands. Using six degree-of-freedom (6DOF) retro-reflective motion capture, Degeorges et al. (2005) reported similar data for six human subjects. Methods used by Uchiyama et al. (2000) created higher loads on the joints than would typically occur during a gentle grasping action; methods used by Degeorges et al. (2005) were affected by skin movement. Excluding these data from an overall magnitude, mean radial/ulnar deviation and pronation/supination among the remaining references were 5.6 and 6.6°, respectively (Table 1). Data on joint translations free from skin movement are also rare. Uchiyama et al. (2000) reported 1 mm movement of the PIP center-of-rotation during F3 flexion. Somewhat related, Miura et al. (2004) reported in vivo translations of 2 mm for the center-of-rotation of the trapeziometacarpal joint.

Previous optical motion capture studies used a single tracking marker on the dorsal aspect of the finger joints, allowing calculation of one and two DOF joint angles. Additional algorithms were needed to estimate joint centers and the palmar surface of the fingers (Lee and Zhang, 2005; Zhang, et al., 2003). To overcome these limitations, we developed a 6DOF model (6DHand) to obtain unconstrained kinematics of finger segments (phalanges) and the hand (aggregate of metacarpals). To evaluate kinematic performance, we hypothesized that accessory motions at the MCP, PIP, and DIP joints would be small (less than 5° rotations, and less than 2 mm translations) if segment anatomical reference frames were aligned correctly, and skin movement artifacts were negligible.

## 2. Methods

Following informed consent approved by the agency Human Subjects Review Board, 20 adults (10 female) were enrolled in the study: mean age, body mass, height, and hand length were 26 years (standard deviation 8), 83 kg (27), 173 cm (11.3), and 18.7 cm (1.2), respectively. After the protocol was explained, motion capture markers were applied (Fig. 1). A static calibration was obtained with the right hand in an anatomically neutral posture (Calibration), from which joint centers, anatomically meaningful axes of rotation (local reference frames, LRFs), and geometric shapes were defined (Fig. 2). Unlike the phalanges defined by frusta of right circular cones, the hand segment is defined as an elliptical cylinder, with

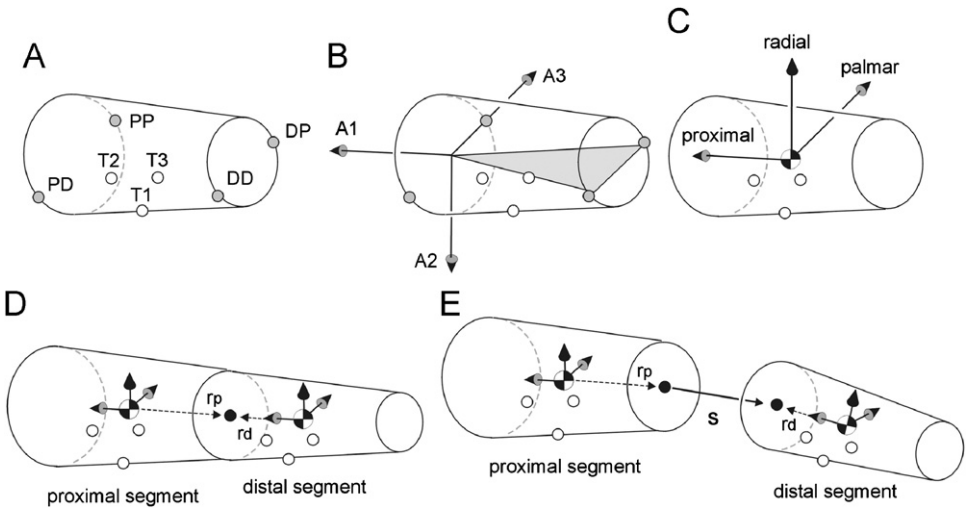


**Fig. 2.** Defining local reference frames (LRFs) and associated kinematics. (A) Anatomical landmarks define the endpoints for a typical phalange (PD, PP=proximal dorsal and palmar joint lines; DD, DP=distal dorsal and palmar joint lines; dorsal tracking markers are also applied (T1–T3). (B) Axis A1 is defined through the segment endpoints, i.e., from midpoint DD–DP to midpoint PD–PP; A2 is perpendicular to a plane defined by DD, DP, and the midpoint of PD–PP; A3 is defined as the cross-product of vectors aligned with A2 and A1. (C) A 90° rotation about A1 aligns A3 with the flexion–extension axis for the preferred Euler rotation sequence (flexion/extension, radial/ulnar deviation, and pronation/supination). The LRF is translated to the center-of-mass of the phalange, defined by its associated frustum; the proportion of the assigned phalange mass to the total hand mass is defined by the proportion of its frustum volume to the total hand volume. Note that PD, PP, DD, and DP are removed during dynamic activities. (D) During subject calibration, the distal endpoint of the proximal segment (black circle) is coincident with the proximal endpoint of the distal segment, defined in each LRF with a local position vector (**rp**, **rd**, dashed lines). (E) During dynamic activities, the local vectors **rp** and **rd** locate different positions in global space, quantifying joint translations; a translation vector (**s**) is defined as the position of the proximal end of the distal segment, with respect to the distal end of the proximal segment, and is represented in the LRF of the proximal segment.

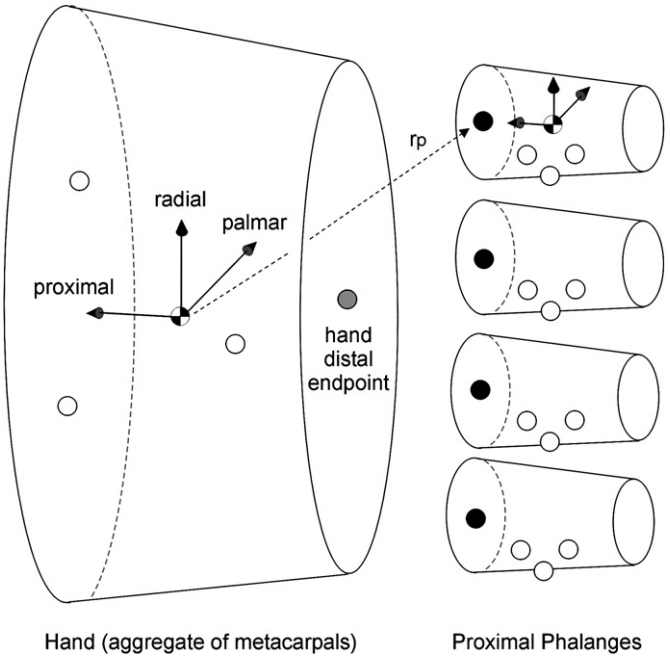


**Fig. 3.** Defining MCP joint translations. Using the distal endpoint of the hand segment (gray circle) to define MCP joint translations would cause spuriously large results. To overcome this, a local position vector (**rp**, dashed line) creates a virtual marker coincident with the proximal endpoint of each proximal phalange (black circles) during subject calibration. During dynamic activities, these local position vectors locate the MCP joints as viewed from the hand segment.

proximal and distal endpoints on the long axis of this cylinder (Fig. 3). In this situation, translations at the MCP joints would be calculated as the distance from the common distal endpoint of the hand (i.e., the midpoint between the second and fifth metacarpal heads) to the proximal endpoint of each proximal phalange and result in spuriously large magnitudes. To overcome this, a local position vector located a virtual marker coincident with the proximal endpoint of each proximal phalange during subject calibration. During dynamic activities, these local position vectors locate the MCP joints as viewed from the hand segment.

Dynamic trials involved lightly gripping a 30 mm diameter cylindrical handle (Natural Grip), wrapped with pressure sensitive film for assessment of contact forces beyond the scope of this paper (Sinsel et al., 2010). This prompted 40–80° of flexion at the MCP, PIP, and DIP joints. Marker trajectories were obtained at 100 Hz using a 14-camera Vicon Nexus system (Oxford Metrics Group, Oxford, England; Table 2); calibration accuracy was on the order of 0.5 mm, for a control volume 1.3 m wide, 1.5 m long, and 1.0 m high. Interpolation and low-pass filtering (6 Hz cutoff) were performed in Visual3D (C-Motion, Inc., Rockville MD, USA). 6DOF joint kinematics were calculated using Visual3D, and averaged across subjects for the sampled frame at the midpoint of the calibration trial (Calibration), and at the midpoint of a nearly static, 5 s, gripping action (Natural Grip). Means and standard deviations were tabulated, and highlighted when they exceeded accessory motion thresholds (5° rotations, 2 mm translations). Rotational and translational kinematics of the thumb were omitted because of skin movement artifacts not yet adequately resolved.

## 3. Results

With a few exceptions, accessory motions were small across all joints during the Calibration and Natural Grip tests (Table 3); 11 of 40 accessory rotations were greater than the 5° threshold, and 8 of 72 accessory translations were greater than the 2 mm threshold. The MCP joint permitted greater pronation than expected at F2 and F3 (Calibration), and greater supination at F3, F4, and F5 (Natural Grip). The PIP joint permitted greater than 5° of supination only at F2 and F3 (Calibration, Natural Grip). The DIP joint permitted greater than 5° of radial deviation only for F5 (Calibration, Natural Grip). Ulnar translations were greater than 2 mm only for F5 MCP (Natural Grip). Proximal translations greater than 2 mm were observed only for the Natural Grip, occurring at all MCP joints (approximately 10 mm each), and F2 PIP, F3 PIP, and F3 DIP (2–3 mm).

## 4. Discussion and conclusions

Overall, the 6DHand performed well for the gripping analyses. Spurious pronation/supination may be related to misaligned LRFs; calibration markers applied to the dorsal and palmar aspects of

**Table 2**
Details of a typical camera configuration.

| Camera | C01 | C02 | C03 | C04 | C05 | C06 | C07 | C08 | C09 | C10 | C11 | C12 | C13 | C14 |
|---|---|---|---|---|---|---|---|---|---|---|---|---|---|---|
| $\Phi$ (deg.) | 7 | 40 | 50 | 60 | 86 | 120 | 120 | 232 | 263 | 288 | 305 | 324 | 337 | 354 |
| $\rho$ (cm) | 260 | 239 | 191 | 165 | 155 | 181 | 117 | 149 | 156 | 187 | 177 | 173 | 245 | 203 |
| $h$ (cm) | 70 | 98 | 164 | 72 | 198 | 175 | 229 | 224 | 143 | 155 | 78 | 156 | 98 | 167 |
| $\theta$ (deg.) | 0 | −10 | −20 | 10 | −35 | −25 | −45 | −40 | −20 | −25 | 0 | −20 | 0 | −20 |
| $F$ (mm) | 20 | 20 | 16 | 12.5 | 16 | 16 | 16 | 12.5 | 12.5 | 16 | 12.5 | 20 | 20 | 16 |

Cameras are Vicon MX-F40 models, with 4.0 megapixel resolution at the 100 Hz frame rate used in this study. The location of the grasped cylindrical handle (approximately waist height) is projected onto the floor, and this point serves as the origin of a cylindrical coordinate system. The positive $x$-, $y$-, and $z$-axes are anterior, lateral to the left, and vertically upward, with respect to the subject who stands near the origin, respectively. $\Phi$ is the rotation about the $z$-axis, $\rho$ is the radial distance to the specific camera, and $h$ is the $z$-coordinate. $\theta$ is the angle the camera's optical axis makes with the horizontal (+ pitch up and − pitch down). $F$ is the focal length of the lens.

**Table 3**
Rotational and translational degrees-of-freedom (labels indicate positive sense for each DOF).

| | Calibration | | | Natural Grip | | |
|---|---|---|---|---|---|---|
| | Flexion (deg.) | Ulnar dev. (deg.) | Pronation (deg.) | Flexion (deg.) | Ulnar Dev. (deg.) | Pronation (deg.) |
| F2 MCP | *−7.8 (7.0)* | *−10.2 (7.4)* | **8.3*** (4.7) | *49.8 (10.7)* | *7.1 (4.9)* | 3.9 (7.0) |
| PIP | *3.3 (8.4)* | 4.8 (3.0) | **−5.1*** (3.3) | *76.4 (4.6)* | 1.7 (3.1) | **−6.8*** (4.2) |
| DIP | *−4.3 (7.4)* | 2.8 (3.5) | 0.5 (0.7) | *38.1 (10.3)* | 1.5 (4.7) | 2.9 (3.2) |
| F3 MCP | *−7.5 (7.2)* | *−2.9 (4.8)* | **7.9*** (4.5) | *67.3 (8.9)* | *4.5 (4.0)* | **−11.8*** (5.9) |
| PIP | *1.8 (10.5)* | 2.7 (2.1) | **−5.3*** (4.0) | *69.7 (5.4)* | 3.6 (4.4) | **−6.9*** (4.0) |
| DIP | *−5.1 (7.6)* | 2.8 (3.3) | 0.0 (0.9) | *47.7 (8.5)* | 0.4 (3.5) | 2.3 (2.6) |
| F4 MCP | *−11.5 (8.6)* | *6.3 (5.2)* | 5.0 (4.0) | *70.9 (9.8)* | *4.9 (4.4)* | **−15.2*** (6.4) |
| PIP | *4.7 (10.3)* | −2.0 (3.4) | −1.0 (3.4) | *66.5 (6.0)* | −0.7 (5.7) | −0.5 (3.2) |
| DIP | *−3.9 (5.5)* | −2.0 (2.5) | 0.1 (0.7) | *44.1 (9.4)* | −1.0 (3.3) | 2.7 (3.0) |
| F5 MCP | *−17.8 (12.8)* | *19.4 (9.2)* | 0.5 (7.8) | *68.7 (11.6)* | *4.3 (6.6)* | **−20.9*** (9.4) |
| PIP | *10.3 (10.0)* | −3.5 (4.0) | −3.0 (4.9) | *50.0 (7.4)* | −2.0 (6.2) | −2.1 (5.7) |
| DIP | *−2.2 (6.0)* | **−5.7*** (3.0) | −1.1 (1.6) | *40.4 (9.0)* | **−5.4*** (3.3) | 1.2 (2.9) |
| | Radial (mm) | Palmar (mm) | Proximal (mm) | Radial (mm) | Palmar (mm) | Proximal (mm) |
| F2 MCP | 0.07 (0.15) | −0.06 (0.42) | −0.03 (0.30) | 1.50 (1.51) | 1.48 (2.49) | **11.15*** (1.90) |
| PIP | 0.00 (0.10) | 0.07 (0.17) | −0.04 (0.13) | −0.21 (0.85) | 1.08 (1.36) | **2.75*** (1.19) |
| DIP | 0.00 (0.08) | 0.02 (0.13) | 0.04 (0.13) | −0.26 (0.46) | −1.26 (0.90) | 1.97 (0.63) |
| F3 MCP | 0.02 (0.13) | 0.03 (0.27) | −0.07 (0.29) | 1.36 (1.11) | 0.34 (2.29) | **9.17*** (2.14) |
| PIP | −0.03 (0.10) | 0.01 (0.11) | 0.02 (0.09) | −1.62 (0.79) | 1.36 (1.17) | **3.04*** (1.13) |
| DIP | 0.02 (0.14) | 0.02 (0.09) | 0.02 (0.07) | −0.72 (0.46) | −0.89 (1.12) | **2.01*** (0.79) |
| F4 MCP | 0.02 (0.15) | −0.06 (0.37) | −0.08 (0.40) | −0.46 (1.86) | 0.96 (2.45) | **8.04*** (2.47) |
| PIP | 0.06 (0.27) | 0.08 (0.20) | −0.01 (0.08) | −0.75 (0.92) | 1.63 (1.13) | 1.49 (0.83) |
| DIP | −0.03 (0.10) | 0.05 (0.10) | 0.03 (0.09) | −0.33 (0.48) | −0.44 (1.10) | 1.76 (0.76) |
| F5 MCP | −0.21 (0.76) | −0.20 (0.63) | −0.15 (0.50) | **−2.45*** (2.24) | 0.65 (3.37) | **8.43*** (2.30) |
| PIP | 0.09 (0.44) | 0.06 (0.20) | −0.04 (0.25) | −0.52 (0.92) | 0.55 (0.80) | −0.09 (1.06) |
| DIP | −0.03 (0.18) | 0.09 (0.16) | 0.04 (0.16) | −0.42 (0.40) | −0.93 (0.60) | 1.36 (0.69) |

Data are means and (standard deviations) for twenty adult subjects, with the fingers neutral (Calibration), and lightly gripping a 30 mm diameter cylindrical handle (Natural Grip). F2, F3, F4 and F5 refer to index, middle, ring, and little fingers, respectively. MCP=metacarpophalangeal joint. PIP/DIP=proximal/distal interphalangeal joints. By definition, translations should be zero for the Calibration trials. Italics entries are considered primary rotations. **Bold asterisks** indicate 11 of 40 accessory rotations $\geq 5^\circ$ and 8 of 72 translations $\geq 2$ mm.

the joint lines were used to define these LRFs, and small placement errors could result in misalignment. A similar situation occurred in clinical gait analysis, where misaligned LRFs in the thigh resulted in cross-talk between knee flexion/extension and adduction/abduction. An optimization procedure was developed to minimize unexpected rotations (Baker et al., 1999; Schache et al., 2006), and could be used if needed, to adjust accessory rotations at the finger joints. Unexpectedly large supination at the MCP joints (greater than 10°) likely reflect the non-rigid behavior of the more proximal hand segment during the gripping action; i.e., the metacarpals tended to cup during this task.

Proximal MCP joint translations were on the order of 10 mm, consistent with skin movement artifact reported by Ryu et al. (2006) for similarly placed markers on the dorsal aspect of the metacarpals. In their magnetic resonance imaging study, skin over the metacarpals moved distally as subjects gripped a 54.3 mm diameter cylinder (range 0.2–9.6 mm, mean 4.5 mm); we would expect larger skin movement in our study, as we used a cylinder approximately half that diameter. Such skin movement would cause the proximal phalanges of the 6DHand to appear to move proximally with respect to the hand segment, just as we observed (Table 3). Translations at the MCP joints would not affect joint kinetics at the DIP, PIP, and MCP joints, as these are calculated from distal to proximal joints (Bresler and Frankel, 1950), and do not require hand kinematics. PIP and DIP translations between 2 and 3 mm are likely due to a combination of misaligned LRFs during calibration, and skin movement during the gripping action.

The 6DHand has the potential to quantify exposures to repetitive stress in a variety of workplace tasks (e.g., typing, small parts assembly, and powered hand tool operation). Coupled with

pressure data mapped to palmar finger surfaces (Sinsel et al., 2010) an approximation of joint kinetics and tissue loads will be possible (Wu et al., 2007), increasing our understanding of the etiology and mitigation of hand or finger disorders. Because the majority of accessory motions (93 of 112) were small in this study, we conclude that this 6DOF approach has potential to appropriately model joints of the fingers while gripping a cylindrical handle. However, this study only assessed performance; rigorous validation of the model will require analyses free from skin movement artifact (e.g., through medical imaging), and are beyond the scope of this short communication.

## Conflict of interest statement

None declared.

## References


Baker, R., Finney, L., Orr, J., 1999. A new approach to determining the hip rotation profile from clinical gait anlaysis data. Hum. Movement Sci. 18, 655–667.

BLS, 2005. Survey of Occupational Injuries and Illnesses. US Department of Labor, Bureau of Labor Statistics, Washington, DC.

Bresler, B., Frankel, J.P., 1950. The forces and moments in the leg during level walking. Trans. ASME January, 27–36.

Chao, E.Y.S., An, K.N., Cooney, W.P., Linscheid, R.L., 1989. Biomechanics of the Hand: A Basic Research Study. World Scientific, Singapore.

Degeorges, R., Oberlin, C., 2003. Measurement of three-joint-finger motions: reality or fancy? A three-dimensional anatomical approach. Surg. Radiol. Anat. 25, 105–112.

Degeorges, R., Laporte, S., Pessis, E., Mitton, D., Goubier, J.-N., Lavaste, F., 2004. Rotations of three-joint fingers: a radiological study. Surg. Radiol. Anat. 26, 392–398.

Degeorges, R., Parasie, J., Mitton, D., Imbert, N., Goubier, J.-N., Lavaste, F., 2005. Three-dimensional rotations of human three-joint fingers: an optoelectronic measurement. Preliminary results. Surg. Radiol. Anat. 27, 43–50.

Kuczynski, K., 1975. Less-known aspects of the proximal interphalangeal joints of the human hand. Hand 7 (1), 31–33.

Lee, S.W., Zhang, X., 2005. Development and evaluation of an optimization-based model for power-grip posture prediction. J. Biomech. 38 (8), 1591–1597.

Liberty-Mutual, 2008. The most disabling workplace injuries cost industry an estimated $48.6 billion. In: Safety, L. M. R. I. f. (Ed.), Workplace Safety Index.

Marras, W.S., Cutlip, R.G., Burt, S.E., Waters, T.R., 2009. National occupational research agenda (NORA) future directions in occupational musculoskeletal disorder health research. Appl. Ergon. 40 (1), 15–22.

Minamikawa, Y., Horii, E., Amadio, P.C., Cooney, W.P., Linscheid, R.L., An, K.-N., 1993. Stability and constraint of the proximal interphalangeal joint. J. Hand Surg. 18A, 198–204.

Miura, T., Ohe, T., Masuko, T., 2004. Comparative in vivo kinematic analysis of normal and osteoarthritic trapeziometacarpal joints. J. Hand Surg. 29A, 252–257.

Netter, F.H., 1991. The CIBA Collection of Medical Illustrations, vol. 8, part 1, p. 73.

NIOSH, 1997. Musculoskeletal Disorders and Workplace Factors. Publication No. 97-141.

Ryu, J.H., Miyata, N., Kouchi, M., Mochimaru, M., Lee, K.H., 2006. Analysis of skin movement with respect to flexional bone motion using MR images of hand. J. Biomech. 39, 844–852.

Sinsel, E.W., Gloekler, D.S., Wimer, B.M., Warren, C., Wu, J.Z., Buczek, F.L., 2010. A novel technique quantifying phalangeal interface pressures at the hand–handle interface. In: Proceedings of the Annual Meeting of the American Society of Biomechanics (ASB), Providence RI, August pp. 18–21.

Schache, A.G., Baker, R., Lamoreux, L.W., 2006. Defining the knee joint flexion–extension axis for purposes of quantitative gait analysis: an evaluation of methods. Gait Posture 24 (1), 100–109.

Uchiyama, S., Cooney, W.P., Linscheid, R.L., Niebur, G., An, K.-N., 2000. Kinematics of the proximal interphalangeal joint of the finger after surface replacement. J. Hand Surg. 25A, 305–312.

Wu, J.Z., Welcome, D.E., Krajnak, K., Dong, R.G., 2007. Finite element analysis of the penetrations of shear and normal vibrations into the soft tissues in a fingertip. Med. Eng. Phys. 29 (6), 718–727.

Zhang, X., Lee, S.W., Braido, P., 2003. Determining finger segmental centers of rotation in flexion–extension based on surface marker measurement. J. Biomech. 36 (8), 1097–1102.